crystals

MDPI

Editorial

Crystal Indentation Hardness

Ronald W. Armstrong [1,*], Stephen M. Walley [2,†] and Wayne L. Elban [3,†]

1 Department of Mechanical Engineering, University of Maryland, College Park, MD 20742, USA
2 Cavendish Laboratory, Madingley Road, Cambridge CB3 0HE, UK; smw14ster@googlemail.com
3 Department of Engineering, Loyola University Maryland, Baltimore, MD 21210, USA; welban@loyola.edu
* Correspondence: rona@umd.edu; Tel.: +1-410-723-4616
† These authors contributed equally to this work.

Academic Editor: Sławomir Grabowski
Received: 5 January 2017; Accepted: 6 January 2017; Published: 12 January 2017

Abstract: There is expanded interest in the long-standing subject of the hardness properties of materials. A major part of such interest is due to the advent of nanoindentation hardness testing systems which have made available orders of magnitude increases in load and displacement measuring capabilities achieved in a continuously recorded test procedure. The new results have been smoothly merged with other advances in conventional hardness testing and with parallel developments in improved model descriptions of both elastic contact mechanics and dislocation mechanisms operative in the understanding of crystal plasticity and fracturing behaviors. No crystal is either too soft or too hard to prevent the determination of its elastic, plastic and cracking properties under a suitable probing indenter. A sampling of the wealth of measurements and reported analyses associated with the topic on a wide variety of materials are presented in the current Special Issue.

Keywords: crystal hardness; nanoindentations; dislocations; contact mechanics; indentation plasticity; plastic anisotropy; stress–strain characterizations; indentation fracture mechanics

1. Introduction

The concept of material hardness has been tracked historically by Walley starting from biblical time and proceeding until the 1950s, with pictorial emphasis given to the earliest 19th century design of testing machines and accumulated measurements [1]. Walley's review leads up to David Tabor setting a new course via science connection with his seminal 1951 book *The Hardness of Metals* [2] and further leading, for example, to a later 1973 conference proceedings on *The Science of Hardness Testing and Its Research Applications* [3]. The subject has gained increased importance with the relatively recent advent of orders of magnitude greater force and displacement measuring capabilities available with modern nano-indentation test systems. A review was presented in 2013 of the complete elastic, plastic and, when appropriate, cracking behaviors that can be monitored for crystals, polycrystals, composites and amorphous materials under suitable probing indentation [4]. A substantial reference list was included in the review of conferences and books produced until that time. As will be seen in the current updated collection of research and review articles, no crystal can be too soft or too hard within its environment to escape measurement with a suitable probing indenter applied using appropriate test conditions.

2. Continuous Indentation Testing

The original application of the hardness test corresponded to the obtainment of a single reference point for measurement of an applied load and resultant plastic deformation. Much has been made, and continues to be made, of correlating the measurement with some aspect of the same material unidirectional stress–strain behavior beginning from historical association with the ultimate

tensile stress. In like manner, current achievements of continuous indentation load–deformation measurements, particularly obtained with nanoindentation test instruments, are being developed to describe the full material indentation-based stress–strain behavior. Figure 1 provides an example in which a number of measurements are compared. The hardness stress is load divided by contact area; and, the hardness strain is based on a spherical-tipped indenter and evaluated in terms of the surface-projected indentation diameter, d, divided by the actual or effective ball diameter, D [5]. The terminal open circle points on the dashed and solid elastic loading lines are computed for indicated D values on the basis of an indentation fracture mechanics description, as will be described. Pathak and Kalidindi have given an updated description of such nanoindentation stress–strain curves [6]. Here, a brief preview is given of information currently available from point-by-point measurements made conventionally or from continuous load/penetration measurements.

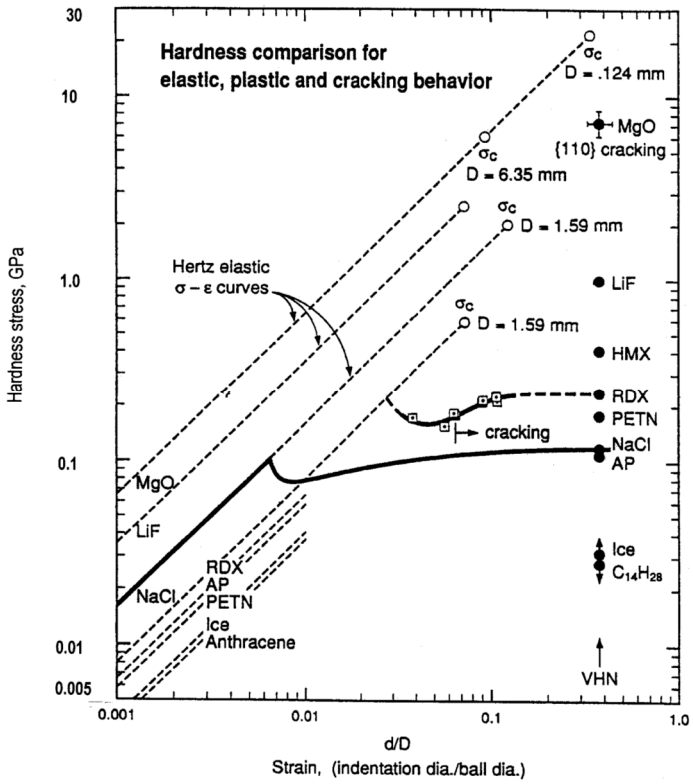

Figure 1. Hardness-based stress–strain description of indentation test measurements. The hardness stress is load divided by the projected area of contact; and, the hardness strain is the projected contact diameter divided by the actual or effective ball diameter of the indenter tip [5]. The solid experimental (ball test) and dashed linear dependencies are computed in accordance with a Hertzian description; and, the Vickers hardness numbers are plotted on the abscissa scale at a position corresponding to the indenter diagonal, $d = 0.375D$.

2.1. Continuous Load–Deformation Measurements

The NaCl crystal (solid curve) hardness stress–strain measurement shown in Figure 1 was obtained on indenting an {001} crystal surface with a 6.35 mm ball in a standard compression test. Such measurments are made much easier with the naturally-rounded tips of nanometer- or micrometer-scale indenter tips in nano-test indentation systems. Figure 2 shows an example elastic loading/unloading behavior recorded for nanoindentation of a {0001} sapphire crystal surface [7]. The nonlinear dependence on penetration depth, h, may be employed to determine the effective elastic modulus for a known tip diameter in accordance with the Hertzian relationship:

$$E^* = [\{(1 - \nu_B)/E_B\} + \{(1 - \nu_S)/E_S\}]^{-1} = (3\sqrt{2}/4)(P/D^{1/2})h^{-3/2} \quad (1)$$

In Equation (1), ν_B, E_B and ν_S, E_S are Poisson's ratio and Young's modulus for ball and specimen, respectively, P is load, and again, D is (effective) ball diameter. As indicated in Figure 2, the value of E^* can be determined from fit to the indentation loading curve if D for the rounded indenter tip is known. Dub, Brazhkin, Novikov, Tolmachova et al. have reported similar measurements on sapphire and stishovite single crystals [8]. Elastic modulus determinations for aluminum have been reported for both micro- and nano-scale test systems [9,10]. Solhjoo and Vakis have provided a molecular dynamics assessment of surface roughness on E^* determinations [11]. The initial loading method compares with an alternative method of determining E^* from an unloading curve after small plastic deformation [12].

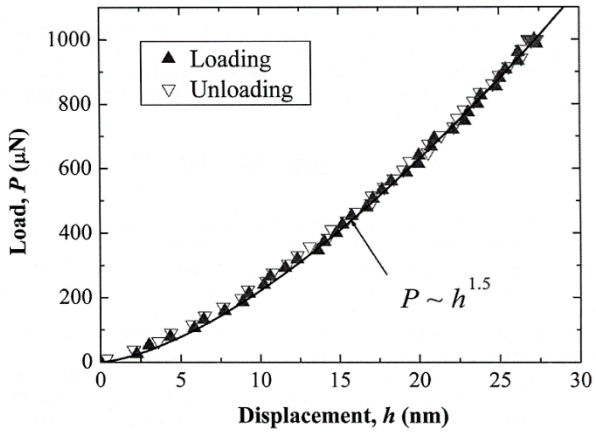

Figure 2. Continuous load/unload curve for nanoindentation of a (0001) sapphire crystal surface [7].

2.2. Crystal Plasticity

The omnipresent elastic loading is eventually interrupted moreso sooner than later by the so-called "pop-in" initiation of crystal plasticity. An example is shown in Figure 3 for the ambient temperature nanoindentation of several different body-centered cubic (bcc) tantalum crystal surfaces [13]. Beyond the higher hardness of the (001) crystal surface, one might note the rapid hardening at the end of the pop-in displacement and the indication of greater strain hardening within the hardened (001) indentation region.

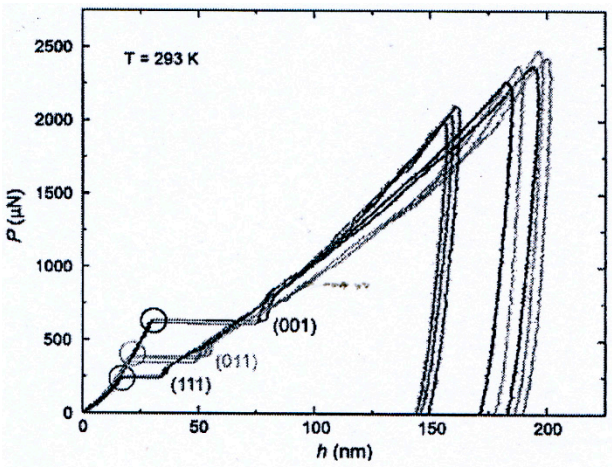

Figure 3. Nanoindentation load–penetration curves obtained with impressing a (rounded point) Berkovich tri-pyramidal indenter into various tantalum (111), (011) and (001) crystal surfaces [13].

Such measurements as shown in Figure 3 have provided valuable information for dislocation mechanics modeling of the crystal deformation behavior, particularly in connection with determining the theoretical shear stress required for dislocation nucleation within a zone below the indentation. Ruestes, Stukowski, Tang, Tramontina et al. have reported on atomic simulation of dislocation creation at nanoindentations in tantalum crystals, including the occurrence of deformation twinning [14]. Alhafez, Ruestes, Gao and Urbassek have investigated nanoindentations made in hexagonal close-packed (hcp) crystal surfaces [15]. A standard (elongated) Knoop indenter system is often employed to evaluate the plastic anisotropy of both ductile and brittle crystal materials [16].

2.3. Crystal Cracking

There are two main aspects of indentation-induced (cleavage) cracking determinations that are of interest: (1) investigation of dislocation mechanism(s) for crack formation; and (2) specification of the indentation fracture mechanics stress intensity for crack propagation.

2.3.1. Crack Formation

Figure 4 provides an example of crack formation at a crystallographically-aligned diamond pyramid indentation impressed into an ammonium perchlorate (AP) {210} crystal surface [17]. The top-side cleavage crack has been generated by sessile dislocations reacted at the intersections of the indicated juxtaposed {111} slip planes, in the same manner reported for cracking at similar indentations put into {001} MgO crystal surfaces and originally proposed for cleavage crack formation in α-iron and other bcc metals [4]. Close examination of the reflected optical image gives an indication that the crack has formed in the valley between otherwise raised surface regions on either side of the indentation. Such "piling up" results from secondary slip occurring to accommodate the primary indentation-forming displacement [4].

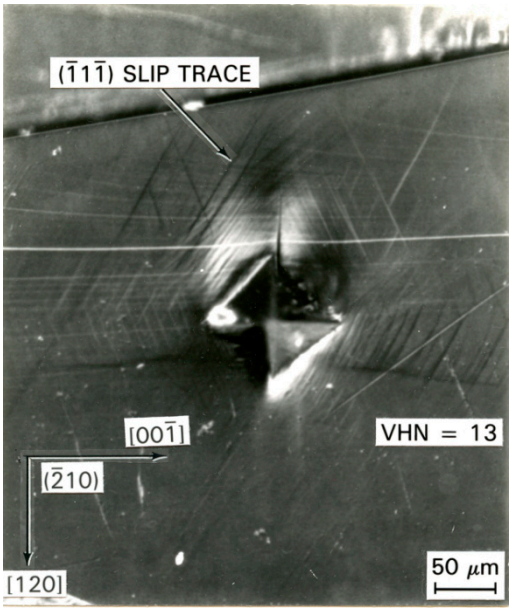

Figure 4. {001} cleavage crack produced by Cottrell-type dislocation reaction at a diamond pyramid indentation impressed into a {210} ammonium perchlorate (AP), NH_4ClO_4, crystal surface [17].

2.3.2. Indentation Fracture Mechanics

An example of elastic, plastic and cracking hardness measurements spanning load and size characterizations for nano- to micro-scale indentations and cracking is shown in Figure 5 [18]. The left-side linear solid and dashed line is the computed Hertzian dependence for elastic behavior,

following a $P \sim d^3$ dependence. The next broad band containing filled circle, triangle and square points applies for the determination of the hardness dependence, with d_i being the indentation diagonal length and is shown to approximate, at higher P value, to a $P \sim d_i^2$ dependence. The open symbols correspond to the shift of the load and diagonal measurements to an effective ball diameter result. The furthest right-side measurements are for an indentation fracture mechanics assessment applied to crack extensions following a theoretical $P \sim d_C^{3/2}$ dependence. The figure indicates that plasticity precedes cracking, in line with other results shown in Figure 1 that also show that cracking requires a higher load at smaller effective ball sizes. Wan, H.; Shen, Y.; Chen, Q. and Chen, Y. have elaborated on the plastic 'damage' preceding such cracking produced in silicon crystals with different type indenters [19]. Vodenitcharova, Borrero-López and Hofffman described the related cracking associated with scratching along different directions on {100} silicon crystal wafers [20]. The hardness literature shows such Griffith-based crack analyses to be widely employed for characterizing the cracking behavior of brittle ceramic and glass materials.

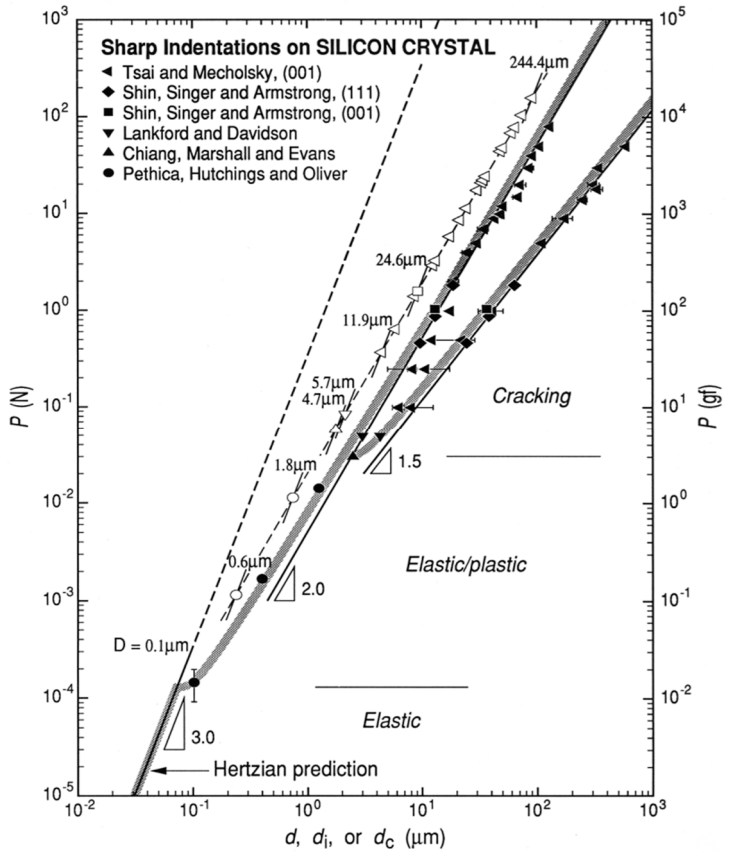

Figure 5. The load, P, versus elastic, d, plastic, d_i, or crack extent, d_c, dependence for cracking of silicon crystal surfaces indented with various sharp indenters [18].

3. Applications

Particular attention was given to example hardness aspects of surface films and coatings in the previous review [4]. Here, we mention, first, an important hardness connection with material compaction behaviors that arise for softer organic crystals relating to pharmaceutical tableting [21] and formulated energetic material processing [5]. Research effort on the former topic has been carried on to investigating temperature [22] and strain rate [23] influences on molecular crystal hardness. In the latter energetic crystal case, a recent report on hardness and molecular dynamics aspects of RDX (cyclotrimethylenetrinitramine) crystals has dealt with concern for their mechanical and tribological properties [24].

Beyond the referenced-above consideration of hardness-determined elastic deformation behavior of sapphire, its hardness properties have been investigated to relate with abrasive wear resistance [25]. Tribological concern has been with chemomechanical aspects of sapphire crystal, polycrystal ZnO coating and other ceramic material hardness properties [26]. In addition, there are interesting optical (cathodoluminescence) properties associated with dislocation zones at nanoindentations in ZnO crystals [27].

3.1. Polycrystals, Polyphases and Amorphous Phases

Particular attention was also directed in [4] to relating hardness properties between individual crystals and their polycrystalline counterparts. The connection was reasonably shown to be well-established in the so-called Hall–Petch (H–P) relationship for hardness:

$$H = H_0 + k_H \ell^{-1/2} \quad (2)$$

In Equation (2), H is Meyers hardness, $P/(\pi d^2/4)$; H_0 is the single crystal hardness; k_H is a microstructural stress intensity; and ℓ is average (crystal) grain diameter, generally measured on a line intercept basis. Other hardness values are easily related to the Meyer hardness.

Equation (2) is related to the same type equation for the true compressive (or tensile) stress (σ_ε)–true strain (ε) behavior for which $k_H \approx 3k_\varepsilon$. Recent estimations have been reported for H–P k values determined for steel materials through nanoindentation measurements [28]. In line with the H–P model description, the obstacle presented to slip penetrations by grain boundaries has been investigated in the bcc metals case by Soer, Aifantis and De Hosson [29] and more recently in (hcp) α-titanium via high resolution X-ray and electron microscope methods [30]. Related hardness and grain size dependent scratch results have been reported for polycrystalline copper [31]. The influence of H–P strengthening of polycrystalline diamond has been described [32] and also for cubic boron nitride via nanotwinned (boundary) strengthening [33].

An important crystal size-dependent connection has been made with composite WC–Co cermet material for which indentations made on the individual components were known to follow separate H–P dependencies [34]. A recent report on the system has been made by Roa, Jimenez–Pique, Verge, Tarragó et al. [35]; see Figure 6. In related work, Roa et al. have determined an intermediate k_H for the combined deformation of phases [36]. Zhang, Wang and Dai have employed nanoindentation testing to investigate the rate dependence of plastic flow in metallic glass materials [37].

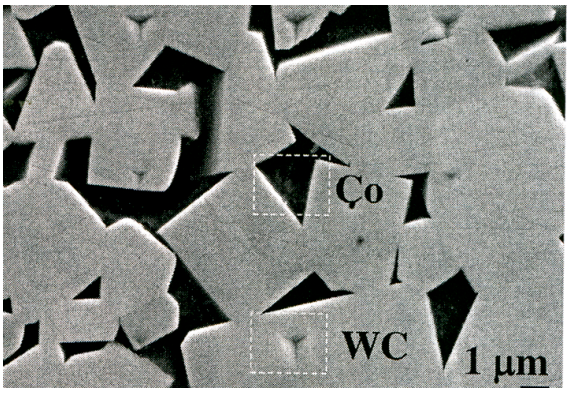

Figure 6. Berkovich nanoindentations made within the WC particle and Co binder phases of the composite cermet material [35].

3.2. Hardness as a Test Probe

In this concluding section, we return to reference [3] in which Gilman pointed to the important use of local hardness testing as a strength microprobe [38] and was able to correlate hardness with a number

of material properties such as yield strength, elastic modulus, glide activation energy and energy gap density for a variety of crystals. The advent of nanoindentation testing has given greater meaning to such probe capability. Emphasis was given previously in [4] to connection with probe aspects of atomic force microscopy for which a new tip fabrication procedure has recently been reported [39]. Another recent application has been to investigate the strain hardening surrounding larger Rockwell indentations made in electrodeposited nanocrystalline nickel material with different grain sizes [40]. Additional examples include (1) investigating shear banding in metallic glass materials [41]; and, nano-probing of diffusion-controlled deformation on a copper crystal surface [42] and on different surfaces of ZnO crystals [43].

4. Summary

An editorial introduction to the Special Issue on crystal indentation hardness has been presented by the authors while building upon their previous review entitled *Elastic, Plastic and Cracking Aspects of the Hardness of Materials* [4]. The wide variation in currently referenced journals gives an indication of the broad interest in the subject. Hopefully, the more recent referenced reports will be viewed as indicating an expanded interest in the topic of crystal hardness testing, particularly as provided in this sampling of important measurements and analyses stemming from current attention being given to all aspects of nanoindentation hardness testing.

Conflicts of Interest: The authors declare no conflict of interest.

References

1. Walley, S.M. Review: Historical origins of indentation hardness testing. *Mater. Sci. Technol.* **2012**, *28*, 1028–1044. [CrossRef]
2. Tabor, D. *The Hardness of Metals*; Clarendon Press: Oxford, UK, 1951.
3. Westbrook, J.H.; Conrad, H. (Eds.) *The Science of Hardness Testing and Its Research Applications*; American Society for Metals: Metals Park, OH, USA, 1973.
4. Armstrong, R.W.; Elban, W.L.; Walley, S.M. Elastic, plastic and cracking aspects of the hardness of materials. *Int. J. Mod. Phys. B* **2013**, *28*, 1330004. [CrossRef]
5. Armstrong, R.W.; Elban, W.L. Review: Hardness properties across multi-scales of applied loads and material structures. *Mater. Sci. Technol.* **2012**, *28*, 1060–1071. [CrossRef]
6. Pathak, S.; Kalidindi, S.R. Spherical nanoindentation stress-strain curves. *Mater. Sci. Eng. R* **2015**, *91*, 1–36. [CrossRef]
7. Lu, C.; Mai, Y.W.; Tam, P.L.; Shen, Y.G. Nanoindentation-induced elastic-plastic transition and size effect in α-Al_2O_3 (0001). *Philos. Mag. Letts.* **2007**, *87*, 409–415. [CrossRef]
8. Dub, S.N.; Braxhkin, V.V.; Novikov, N.V.; Tolmachova, G.N.; Litvin, P.M.; Litagina, L.M.; Dyuzheva, T.I. Comparative Studies of Mechanical Properties of Stishovite and Sapphire Single Crystals by Nanoindentation. *(RU) J. Superhard Mater.* **2010**, *32*, 406–414. [CrossRef]
9. Ferrante, L., Jr.; Armstrong, R.W.; Thadhani, N.N. Elastic/plastic deformation behavior in a continuous ball indentation test. *Mater. Sci. Eng. A* **2004**, *371*, 251–255. [CrossRef]
10. Yoshida, M.; Sumomogi, T.; Endo, T.; Maeta, H.; Kino, T. Nanoscale Evaluation of Strength and Deformation Properties of Ultrahigh-Purity Aluminum. *(JPN) Mater. Trans.* **2007**, *48*, 1–5. [CrossRef]
11. Solhjoo, S.; Vakis, A.I. Continuum mechanics at the atomic scale: Insights into non-adhesive contacts using molecular dynamics simulations. *J. Appl. Phys.* **2016**, *120*, 215102. [CrossRef]
12. Oliver, W.C.; Pharr, G.M. An improved technique for determining hardness and elastic modulus using load and displacement sensing indentation experiments. *J. Mater. Res.* **1992**, *7*, 1564–1583. [CrossRef]
13. Alcala, J.; Dalman, R.; Franke, O.; Biener, M.; Biener, J.; Hodge, A. Planar defect nucleation and annihilation mechanisms in nanocontact plasticity of metal surfaces. *Phys. Rev. Lett.* **2010**, *109*, 075502. [CrossRef] [PubMed]

14. Ruestes, C.J.; Sukowski, A.; Tang, Y.; Tramontina, D.R.; Erhart, P.; Remington, B.A.; Urbassek, H.M.; Meyers, M.A.; Bringa, E.M. Atomistic simulation of tantalum nanoindentation: Effects of indenter diameter, penetration velocity, and interatomic potentials on defect mechanisms and evolution. *Mater. Sci. Eng. A* **2014**, *613*, 390–403. [CrossRef]
15. Alhafez, I.A.; Ruestes, C.J.; Gao, Y.; Urbassek, H.M. Nanoindentation of hcp metals: A comparative simulation study of the evolution of dislocation networks. *Nanotechnology* **2016**, *27*, 045706. [CrossRef] [PubMed]
16. Gao, F. Theoretical model of hardness anisotropy in brittle materials. *J. Appl. Phys.* **2012**, *112*, 023506. [CrossRef]
17. Elban, W.L.; Armstrong, R.W. Plastic anisotropy and cracking at hardness impressions in single crystal ammonium perchlorate. *Acta Mater.* **1998**, *46*, 6041–6052. [CrossRef]
18. Armstrong, R.W.; Ruff, A.W.; Shin, H. Elastic, plastic and cracking indentation behavior of silicon crystals. *Mater. Sci. Eng. A* **1996**, *209*, 91–96. [CrossRef]
19. Wan, H.; Shen, Y.; Chen, Q.; Chen, Y. A plastic damage model for finite element analysis of cracking of silicon under indentation. *J. Mater. Res.* **2010**, *25*, 2224–2237. [CrossRef]
20. Vodenitcharaova, T.; Borrero-López, O.; Hoffman, M. Mechanics prediction of the fracture pattern on scratching wafers of single crystal silicon. *Acta Mater.* **2012**, *60*, 4448–4460. [CrossRef]
21. Egart, M.; Janković, B.; Srčič, S. Application of instrumented nanoindentation in preformulation studies of pharmaceutical active ingredients and excipients. *Acta Pharm.* **2016**, *66*, 303–330. [CrossRef] [PubMed]
22. Mohamed, R.M.; Mishra, M.K.; Al-Harbi, L.M.; Al-Ghamdi, M.S.; Asiri, A.M.; Reddy, C.M.; Ramamurty, U. Temperature Dependence of Mechanical Properties in Molecular Crystals. *Cryst. Growth Des.* **2015**, *15*, 2474–2479. [CrossRef]
23. Raut, D.; Kiran, M.S.R.N.; Mishra, M.K.; Asiri, A.M.; Ramamurty, U. On the loading rate sensitivity of plastic deformation in molecular crystals. *CrystEngComm* **2016**, *18*, 3551–3555. [CrossRef]
24. Weingarten, N.S.; Sausa, R.C. Nanomechanics of RDX Single Crystals by Force-Displacement Measurements and Molecular Dynamics Simulations. *J. Phys. Chem. A* **2015**, *119*, 9338–9351. [CrossRef] [PubMed]
25. Voloshin, A.V.; Dolzhenkova, E.F.; Litvinov, L.A. Anisotropy of Deformation and Fracture Processes in Sapphire Surface. *(RU) J. Superhard Mater.* **2015**, *37*, 341–345. [CrossRef]
26. Bull, S.J.; Moharrami, N.; Hainsworth, S.V.; Page, T.F. The origins of chemomechanical effects in the low-load indentation hardness and tribology of ceramic materials. *J. Mater. Sci.* **2016**, *51*, 107–125. [CrossRef]
27. Juday, R.; Silva, E.M.; Huang, J.Y.; Caldas, P.G.; Prioli, R.; Ponce, F.A. Strain-related optical properties of ZnO crystals due to nanoindentation on various surface orientations. *J. Appl. Phys.* **2013**, *113*, 183511. [CrossRef]
28. Seok, M.-Y.; Choi, I.-C.; Moon, J.; Kim, S.; Ramamurty, U.; Jang, J.-I. Estimation of the Hall–Petch strengthening coefficient of steels through nanoindentation. *Scr. Mater.* **2014**, *87*, 49–52. [CrossRef]
29. Soer, W.A.; Aifantis, K.E.; de Hosson, J.T.M. Incipient plasticity during nanoindentation at grain boundaries in body-centered cubic metals. *Acta Mater.* **2005**, *53*, 4665–4676. [CrossRef]
30. Guo, Y.; Collins, D.M.; Tarleton, E.; Hofmann, F.; Tischler, J.; Liu, W.; Xu, R.; Wilkinson, A.J.; Britton, T.B. Measurements of stress fields near a grain boundary: Exploring blocked arrays of dislocations in 3D. *Acta Mater.* **2015**, *96*, 229–236. [CrossRef]
31. Kareer, A.; Hou, X.D.; Jennett, N.M.; Hainsworth, S.V. The interaction between lateral size effect and grain size when scratching polycrystalline copper using a Berkovich indenter. *Philos. Mag.* **2016**, *96*, 3414–3429. [CrossRef]
32. Xu, B.; Tian, Y. Ultrahardness: Measurement and Enhancement. *J. Phys. Chem.* **2015**, *119*, 5633–5638. [CrossRef]
33. Li, B.; Sun, H.; Chen, C. Large indentation strain stiffening in nanotwinned cubic boron nitride. *Nat. Commun.* **2014**, *5*, 4965–4971. [CrossRef] [PubMed]
34. Lee, H.C.; Gurland, J. Hardness and deformation of cemented tungsten carbide. *Mater. Sci. Eng.* **1978**, *33*, 125–133. [CrossRef]
35. Roa, J.J.; Jiménez-Pique, E.; Verge, C.; Tarragó, J.M.; Mateo, A.; Llanes, L. Intrinsic hardness of constitutive phase in WC–Co composites: Nanoindentation testing, statistical analysis, WC crystal orientation effects and flow stress for the constrained metallic binder. *J. Eur. Ceram. Soc.* **2015**, *35*, 3419–3425. [CrossRef]

36. Roa, J.J.; Jiménez-Pique, E.; Tarragó, J.M.; Sandoval, D.A.; Mateo, A.; Fair, J.; Llanes, L. Hall–Petch strengthening of the constrained metallic binder in WC–Co cemented carbides: Experimental assessment by means of massive nanoindentation and statistical analysis. *Mater. Sci. Eng. A* **2016**, *676*, 487–491. [CrossRef]
37. Zhang, M.; Wang, Y.J.; Dai, L.H. Correlation between strain rate sensitivity and α relaxation of metallic glasses. *AIP Adv.* **2016**, *6*, 075022. [CrossRef]
38. Gilman, J.J. Hardness—A Strength Microprobe. In *The Science of Hardness Testing and Its Research Applications*; Westbrook, J.H., Conrad, H., Eds.; American Society for Metals: Metals Park, OH, USA, 1973; pp. 51–74.
39. Göring, G.; Dietrich, P.-I.; Blaicher, M.; Sharma, S.; Korvink, J.G.; Schimmel, T.; Koos, C.; Hölscher, H. Tailored probes for atomic force microscopy fabricated by two-photon polymerization. *Appl. Phys. Lett.* **2016**, *109*, 063101. [CrossRef]
40. Tang, B.T.F.; Zhou, Y.; Zabev, T. Reduced hardening of nanocrystalline nickel under multiaxial indentation loading. *J. Mater. Res.* **2015**, *30*, 3528–3541. [CrossRef]
41. Wang, J.Q.; Perepezko, J.H. Focus: Nucleation kinetics of shear bands in metallic glass. *J. Chem. Phys.* **2016**, *145*, 211803. [CrossRef]
42. Samanta, A.; Weinan, E. Interfacial diffusion aided deformation during nanoindentation. *AIP Adv.* **2016**, *6*, 075002. [CrossRef]
43. Lin, P.H.; Du, X.H.; Chen, Y.H.; Chen, H.C.; Huang, J.C. Nano-scaled diffusional or dislocation creep analysis of single-crystal ZnO. *AIP Adv.* **2016**, *6*, 095125. [CrossRef]